Relations between the Sudbury Neutrino Observatory and the Super Kamiokande solar neutrino rates

Waikwok Kwong and S. P. Rosen
Department of Physics, University of Texas at Arlington, Arlington, Texas 76019-0059
(Received 13 February 1996)

We develop a model-independent method for analyzing the SNO and Super Kamiokande solar neutrino experiments simultaneously, and for establishing relations between them. Representing the rates for the two experiments by a point in a two-dimensional rate-space diagram, we determine the regions of the diagram corresponding to different solutions of the solar neutrino problem. We can then use the method to ascertain which theoretical hypotheses are consistent with the observed rates. [S0556-2821(96)04815-1]

PACS number(s): 26.65.+t, 14.60.Pq

Two high statistics solar neutrino experiments will be coming on line in the near future. Super Kamiokande (SK) [1] expects to begin taking data in April of 1996, and the Sudbury Neutrino Observatory (SNO) [2] in November 1996. Both experiments will observe only the ^{8}B neutrinos, and they will provide accurate determinations of the solar neutrino interaction rates.

Here, we develop a simple, model-independent method for analyzing the rates of the two solar neutrino experiments simultaneously. It will show us immediately whether the observed rates are, or are not, consistent with various theoretical hypotheses for solar neutrinos, in particular Mikheyev-Smirnov-Wolfenstein (MSW) and ''Just-So'' neutrino oscillations. Where different interpretations overlap, it will obviously be necessary to examine more detailed data, such as the recoil electron spectra [3], to resolve ambiguities. We begin by deriving model-independent inequalities between the SNO and Super Kamiokande rates using a technique devised earlier [4].

Super Kamiokande can detect all three flavors of neutrinos through elastic scattering with atomic electrons, $\nu e \rightarrow \nu e$. The correlation between the electron and the neutrino energies is poor because high energy neutrinos can produce soft scattered electrons. One of the principal reactions at SNO is the charged-current process $\nu_e d \rightarrow ppe$, which is sensitive only to ν_e. The correlation between the electron and neutrino energy is much better than that of the elastic scattering—since the two-proton system is relatively heavy, the electron tends to carry off most of the neutrino energy.

A general expression for total rates can be written in terms of the ^{8}B flux $\phi(E_\nu)$ from the standard solar model (SSM), an electron-neutrino ''survival probability'' $P(E_\nu)$, and an experimental cross section σ as

$$R = \int P(E_\nu)\phi(E_\nu)\sigma(E_\nu)dE_\nu . \tag{1}$$

The function $P(E_\nu)$ parametrizes any, possibly energy-dependent, difference between the SSM flux and the one that is actually measured on Earth. These include overall reduction of neutrino fluxes due to solar physics and energy-dependent loss of flux due to oscillations into sterile neutrinos. All experimental parameters are hidden in the cross section σ which involves a convolution over an energy resolution function, a detection efficiency, and the theoretical cross section. The electron energy resolution for SNO is rather close to that of Super Kamiokande, $\Delta E/E$ at 10 MeV is about 10–12 %. The detection efficiency above trigger threshold is very close to 100% for both experiments. In this analysis we will use the same parameters for both experiments: 11% for the energy resolution and a perfect efficiency with a 5 MeV trigger threshold. For the $\nu_e d$ theoretical cross section, we use the result of Ref. [5].

Since the functions $\phi\sigma(E_\nu)$ are known quantities in both experiments, we compare their shapes by defining

$$f_{\mathrm{SK}}(E_\nu) \equiv \frac{\phi\sigma(\nu_e e, E_\nu)}{\int \phi\sigma(\nu_e e, E_\nu)dE_\nu},$$

$$f_{\mathrm{SNO}}(E_\nu) \equiv \frac{\phi\sigma(\mathrm{SNO}, E_\nu)}{\int \phi\sigma(\mathrm{SNO}, E_\nu)dE_\nu}, \tag{2}$$

which are plotted in Fig. 1. Now, let us write

$$f_{\mathrm{SK}}(E_\nu) = \alpha f_{\mathrm{SNO}}(E_\nu) + r(E_\nu), \tag{3}$$

and maximize the constant α subject to the condition that the remainder function $r(E_\nu)$ be everywhere positive. The value obtained, $\alpha = 0.57$, is mainly controlled by the behavior of the cross sections at the upper end of the ^{8}B spectrum: the cross section for elastic νe scattering rises linearly with the neutrino energy, but that for the charged-current interaction at SNO rises much more quickly. A consequence of this behavior is that variations at the low energy end, such as changes in the trigger thresholds and efficiencies, have no effect on α to first order; they affect α only indirectly through a small change in the normalization of $\phi\sigma$. This can be seen in Table I, where we have listed the values of α for different energy resolutions for the two experiments.

Now, we drop the term $r(E_\nu)$, multiply both sides of Eq. (3) with $P(E_\nu)$, and integrate over E_ν. This gives us an inequality between the total rates of the two experiments. Recognizing the denominators in Eq. (2) to be the respective SSM rates, we express the inequality in terms of the ratios of observed to SSM event rates for either oscillations of solar

 © 1996 The American Physical Society

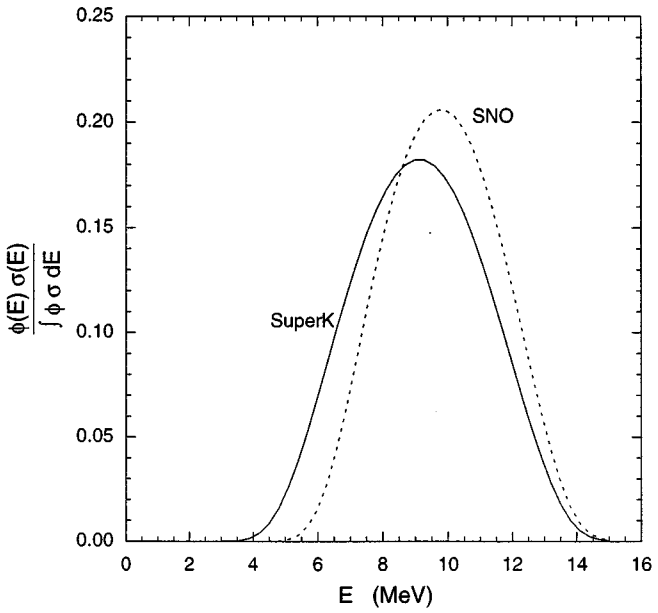

FIG. 1. The normalized shapes of $\phi\sigma$ for SNO and Super Kamiokande.

ν_e into sterile neutrinos, or for an energy-dependent reduction of the solar ν_e flux. We define, for Super Kamiokande and SNO,

$$y \equiv \frac{R(\mathrm{SK})}{R_{\mathrm{SSM}}(\mathrm{SK})}, \quad x \equiv \frac{R(\mathrm{SNO})}{R_{\mathrm{SSM}}(\mathrm{SNO})}, \tag{4}$$

and obtain our first inequality:

$$\text{(I)} \qquad y \geq \alpha x. \tag{5}$$

Next, let us consider the case of oscillations of ν_e into an active neutrino, i.e., ν_μ or ν_τ. The rate for SNO remains unchanged, but that for Super Kamiokande must be modified by the additional neutral-current scattering contributions coming from ν_μ and ν_τ:

$$\begin{aligned} R(\mathrm{SK}) &= \int [P\phi\sigma(\nu_e e, E_\nu) + (1-P)\phi\sigma(\nu_\mu e, E_\nu)]\, dE_\nu \\ &= \int [0.85P(E_\nu) + 0.15]\phi\sigma(\nu_e e, E_\nu)\, dE_\nu, \end{aligned} \tag{6}$$

where $\sigma(\nu_\mu e, E_\nu)$ is the common cross section for $\nu_\mu e$ and $\nu_\tau e$ scattering. To obtain the second line, we have made the substitution $\sigma(\nu_\mu e, E_\nu) = 0.15\sigma(\nu_e e, E_\nu)$, which is a very good approximation in the energy range under consideration

TABLE I. Dependence of α on the energy resolution of SNO and Super Kamiokande.

		SNO resolution		
		0.10	0.11	0.12
SK	0.10	0.569	0.575	0.581
resolution	0.11	0.566	0.572	0.578
	0.12	0.563	0.569	0.575

[6]. It allows us to write the ratio of the actual Super Kamiokande rate to the SSM prediction in the general form

$$y = (1-\beta)\int P(E_\nu) f_{\mathrm{SK}}(E_\nu)\, dE_\nu + \beta, \tag{7}$$

$$\beta = \begin{cases} 0 & \text{oscillation into sterile neutrinos,} \\ 0.15 & \text{oscillation into active neutrinos.} \end{cases} \tag{8}$$

Making use of Eq. (3), we find the general inequality

$$y \geq (1-\beta)\alpha x + \beta \tag{9}$$

which includes Eq. (5) when $\beta = 0$, and gives us our second inequality

$$\text{(II)} \qquad y \geq 0.85\alpha x + 0.15 \tag{10}$$

for oscillations into active neutrino species when $\beta = 0.15$.

The inequalities (I) and (II) are represented graphically in Fig. 2 with the ratio y as ordinate and the ratio x as abscissa. Combinations of observations from the two experiments can be represented by points in the diagram; when experimental errors are taken into account, the points become regions.

Inequality (I) requires that all observed regions lie above the line $y = \alpha x$, $(\alpha = 0.57)$. Since this inequality has been derived under general conditions with few assumptions regarding solar or neutrino physics, all points below the line are unphysical. Put another way, experimental observations falling below the line would imply a fundamental error in present theories of the Sun and solar neutrinos.

Inequality (II) defines a region above the line $y = 0.85\alpha x + 0.15$ $(\alpha = 0.57)$, which is displaced vertically above $y = \alpha x$ by 0.15 and has a 15% smaller slope. All points above this line are consistent with all solutions to the solar neutrino problem, solar physics, and oscillations into active or sterile neutrinos. Points lying between the two lines are consistent with solar physics and oscillations into sterile neutrinos; therefore, should the results from Super Kamiokande and SNO fall within this region, we will be able to rule out oscillations into active neutrinos and predict a smaller neutral-current signal in SNO than that expected in the SSM.

We can represent the present measurements from Kamiokande II, namely, $y = 0.51 \pm 0.07$ as a horizontal band in the diagram. Within statistical fluctuations, the observations from Super Kamiokande are expected to fall inside this band.

There are various fits [7–11] to the existing solar neutrino data based upon the MSW mechanism and the Just-So oscillations, and it is useful to see how they are represented in our plot. The ''small angle'' MSW solution can be characterized by an electron survival probability

$$P(E_\nu) = e^{-C/E_\nu}, \tag{11}$$

where the constant C is proportional to the product of $\sin^2 2\theta$ times Δm^2 and is close to 10 MeV in magnitude. In the standard Δm^2–$\sin^2 2\theta$ oscillation parameter space, the allowed small-angle region can be represented in a log-log plot of constant-probability (or constant-rate) contours by a series of parallel lines, each corresponding to a different value for the product $\Delta m^2 \sin^2 2\theta$; in our Super Kamiokande vs SNO

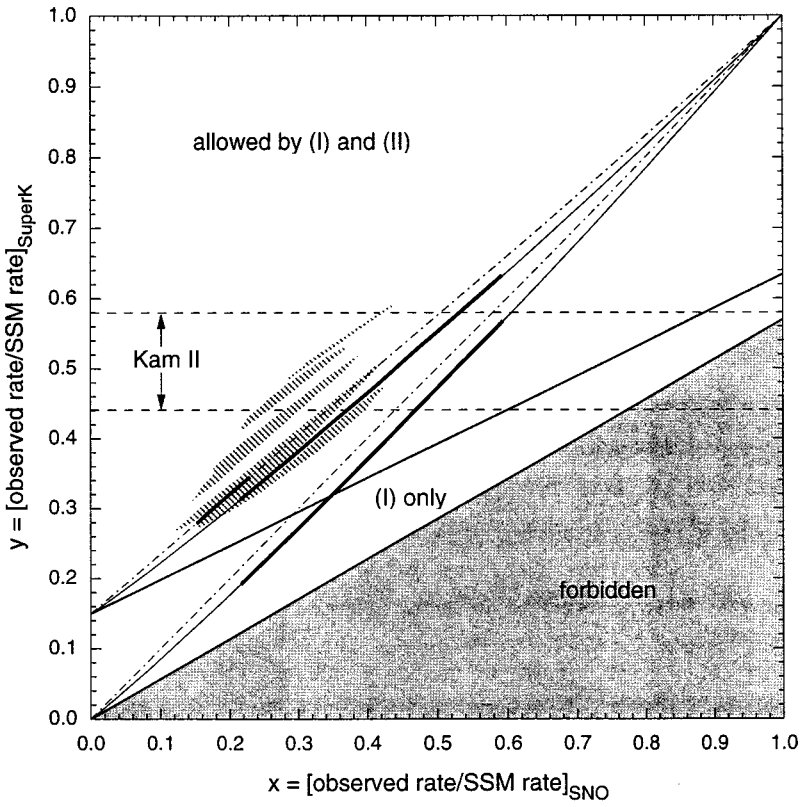

FIG. 2. The MSW solutions in the Super Kamiokande-SNO rate space. The inequalities (I) and (II) divide the rate space into three regions labeled ''allowed by both (I) and (II),'' allowed by ''(I) only,'' and ''forbidden.'' The small-angle MSW solution must lie on the solid thin lines and the large-angle solution must lie on the dot-dashed lines. The upper pair is for oscillation into active neutrinos and the lower pair for sterile neutrinos. Bounds from existing data are represented by the heavy black lines. The patches of shaded areas are bounds from the Just-So solution, shown here for comparison.

rate plot, each of these lines maps into a single point in the x-y rate space, which represents a specific rate for each experiment. As we move from one line to another in the parameter space, the single points in rate space map out a line. To a good approximation, this is a straight line of the form

$$y=(1-\beta)Bx+(1-\beta)A+\beta, \tag{12}$$

where A and B are calculable constants.

The appropriate lines evaluated using Eq. (11) are shown in Fig. 2 as thin solid lines passing through the point (1,1), as required. The upper line ($\beta=0.15$) is for oscillation into active neutrinos and the lower line ($\beta=0$) is for oscillation into sterile neutrinos. These two lines are only very slightly curved, indicating that the linear approximation is valid for a range of values for C in the neigborhood of 10 MeV.

The ''large angle'' MSW solution has an electron-neutrino survival probability

$$P(E_\nu)=\sin^2\theta \tag{13}$$

which is independent of energy and Δm^2. Thus, it maps vertical lines in parameter space into single points in rate space, and as we move from one line to another the points in rate space trace a line. Using the above survival probability in the expression for x and y, we obtain the equation of the line as

$$y=(1-\beta)x+\beta. \tag{14}$$

It is a straight line that always passes through the point (1,1) corresponding to no oscillation, and becomes $y=x$ in the sterile case ($\beta=0$). It is plotted in Fig. 2 as the dot-dashed lines for the active and sterile cases.

In the Just-So solution, the electron neutrino survival probability is given by

$$P(E_\nu)=1-\sin^2 2\theta\sin^2\left(\frac{\Delta m^2 L}{4E_\nu}\right). \tag{15}$$

The value of Δm^2 must be chosen to yield an oscillation length of the same order as the Earth–Sun distance L. Thus, for some energy E_0 within the spectrum of solar neutrinos

$$\frac{\Delta m^2 L}{4E_0}=(n+\tfrac{1}{2})\pi. \tag{16}$$

Letting $\Delta m^2=A\times 10^{-11}$ eV^2 and measuring E_ν in MeV, we can express the y and x coordinates as

$$y=1-(1-\beta)\sin^2 2\theta\int \sin^2\left(\frac{1.90A}{E_\nu}\right)f_{\rm SK}dE_\nu, \tag{17}$$

$$x=1-\sin^2 2\theta\int \sin^2\left(\frac{1.90A}{E_\nu}\right)f_{\rm SNO}dE_\nu. \tag{18}$$

For specific values of Δm^2, or of A, the two integrals can be integrated numerically. Again, eliminating $\sin^2 2\theta$ from the two equations gives us a linear relationship between x and y. As $\sin^2 2\theta$ is varied from 0 to 1, the point (x,y) traces a straight line starting from (1,1) and ends at a point (x_0,y_0) with $x_0>0$ and dependent on the value of Δm^2. By varying also Δm^2, the entire parameter space is mapped into finite regions in Fig. 3: oscillations into active neutrinos give rise to the area enclosed by the solid curve and oscillations into sterile neutrinos give rise to the one enclosed by the dotted

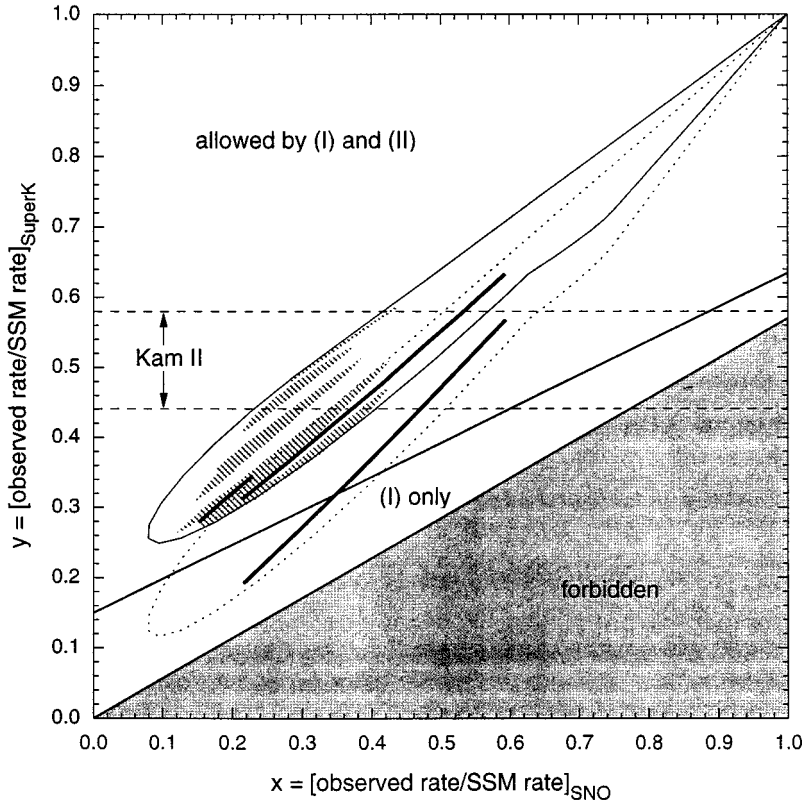

FIG. 3. The Just-So solutions in the Super Kamiokande-SNO rate space. The regions bounded by the thin solid and dotted curves are the solution spaces for Just-So oscillations into active and sterile neutrinos, respectively. See also Fig. 2.

curve. A point falling outside these two regions cannot be explained using the Just-So oscillations.

So far, these lines and closed regions we have discussed represent the entire parameter space within the individual approximations. Existing data from Kamiokande II, the Chlorine experiment, and the two gallium experiments GALLEX and SAGE favor certain ranges of the oscillation parameters. For this we use the global fit of Ref. [9] for the small- and large-angle MSW solutions (the large-angle solution for sterile neutrinos has been ruled out according to this fit) and the result of Ref. [10] for the Just-So solution (depending on how the fitting is done, the sterile case can also be ruled out here, see [10] for details). Both analyses took into consideration theoretical uncertainties. The allowed regions at 95% confidence from these constraints on the SNO and Super Kamiokande rates are shown in both Figs. 2 and 3 as heavy black lines and shaded patches.

It is apparent from Fig. 3 that the theoretical interpretation of some part of the rate-space diagram will be ambiguous. In this case it will be necessary to examine the spectra of recoil electrons observed in both Super Kamiokande and SNO. Although the differences tend to be rather subtle, the combination of high statistics and the ''normalized spectral ratio'' method [3] should enable us to distinguish between active and sterile neutrinos. In addition, the Just-So solution is much more sensitive to the BOREXINO experiment [12] than to either Super Kamiokande or SNO because of the monenergetic ^{7}Be lines. This should help us separate the Just-So oscillations from the MSW solutions.

In conclusion, we have presented a simple model-independent method for looking at the rates for Super Kamiokande and SNO together. Our method enables us to see immediately whether the data are consistent with various theoretical scenarios. We want to emphasize that the experiments must be considered together in order to extract model-independent information: one rate by itself can be consistent with several models and the second rate is needed to reduce ambiguities. Where ambiguities continue to exist, detailed studies of recoil spectra should remove them.

This work was supported in part by the U.S. Department of Energy Grant No. DE-FG03-96ER40943. The authors would like to thank Gene Beier and Hank Sobel for providing the experimental parameters for SNO and Super Kamiokande. One of the authors (S.P.R.) would like to thank Geoffrey West and the Los Alamos National Laboratory for their hospitality at the Summer Workshop and Plamen Krastev for a conversation which initiated this work.

[1] Y. Totsuka, ''Super Kamiokande,'' University of Tokyo Report No. ICRR-227-90-20, 1990 (unpublished).

[2] G. T. Ewan *et al.*, ''Sudbury Neutrino Observatory Proposal,'' Report No. SNO-87-12, 1897 (unpublished); ''Scientific and Technical Description of the Mark II SNO Detector,'' edited by E. W. Beier and D. Sinclair, Report No. SNO-89-15, 1989 (unpublished).

[3] Waikwok Kwong and S. P. Rosen, Phys. Rev. D **51**, 6159

(1995).
[4] Waikwok Kwong and S. P. Rosen, Phys. Rev. Lett. **73**, 369 (1994).
[5] F. J. Kelly and H. Überall, Phys. Rev. Lett. **16**, 145 (1966); S. D. Ellis and J. N. Bahcall, Nucl. Phys. **A114,** 636 (1968).
[6] See, e.g., J. N. Bahcall, *Neutrino Astrophysics* (Cambridge University Press, Cambridge, England, 1989), Sec. 8.2, p. 214–243.
[7] GALLEX Collaboration, P. Anselmann *et al.*, Phys. Lett. B **285**, 390 (1992).
[8] V. Barger, R. J. N. Phillips, and K. Whisnant, Phys. Rev. Lett. **69**, 3135 (1992).
[9] N. Hata and P. Langacker, Phys. Rev. D **50**, 632 (1994).
[10] P. I. Krastev and S. T. Petcov, Phys. Rev. Lett. **72**, 1960 (1994).
[11] J. N. Bahcall and P. I. Krastev, Phys. Rev. D **53**, 4211 (1996).
[12] C. Arpesella *et al.*, ''The BOREXINO Proposals,'' Vol. 1 and 2, edited by G. Bellini *et al.*, University of Milano Report, 1992 (unpublished); R. S. Raghavan, Science **267**, 45 (1995).